High-Density, Large-Area Single-Walled Carbon Nanotube Networks on Nanoscale Patterned Substrates

Yung Joon Jung,* Yoshikazu Homma,*,† Toshio Ogino,† Yoshihiro Kobayashi,† Daisuke Takagi,‡ Bingqing Wei, Robert Vajtai, and Pulickel M. Ajayan

Department of Materials Science and Engineering, Rensselaer Polytechnic Institute, Troy, New York 12180-3590, and NTT Basic Research Laboratories, Atsugi, Kanangawa 243-0198, Japan

Received: March 13, 2003; In Final Form: May 6, 2003

High-density single-walled carbon nanotubes forming self-directed networks on nanoscale patterned substrates are produced by chemical vapor deposition. The roles of catalyst particles for the growth of single-walled carbon nanotubes are investigated. Transition-metal particles of 3−7 nm size, obtained by depositing thin catalyst films (0.5−1 nm), remain as active catalysts for the growth of high-density single-walled carbon nanotubes on select catalyst supports (SiO_2). Highly organized single-walled carbon nanotube architectures with controlled density can be fabricated following the predefined submicrometer-sized substrate patterns, suggesting the possibility of building nanotube-based molecular-scale electronic devices.

1. Introduction

The unique electronic and mechanical properties of carbon nanotubes offer enormous potential for various applications.[1−5] The most promising applications of nanotubes are those involving use in nanoelectronics such as a field effect transistor,[6−9] nanotube interconnects,[10−12] and nanosensors[13] by virtue of their specific electronic structures and transport properties (high current density up to 10^9 A/cm^2 and ballistic conductance)[14,15] with their smaller dimensions. However, for building integrated self-assembled nanotube-based systems, it is required to controllably produce high-density single-walled carbon nanotube (SWNT) networks on a large scale. There have been previous reports about the patterned growth of single-walled carbon nanotubes on the predesigned substrates. In particular, Dai et al.[16,17] showed self-directed growth of suspended nanotube networks on 10 μm silicon tower tops having a liquid-phase catalyst precursor by chemical vapor deposition (CVD). Also recently Homma et al.[18] demonstrated building suspended carbon nanotube networks on 100 nm scale silicon pillar structures by simply depositing a catalyst film on the silicon substrate. These are indeed effective ways to control the growth of carbon nanotubes. However, for the actual application of such self-assembled single-walled carbon nanotube networks, additional efforts to build highly dense and organized nanotube networks connecting all designed locations even on a large scale are required.

In this work we present a further enhanced method to build high-yield growth of single-walled carbon nanotube architectures forming fully bridged networks between patterned structures by controlling CVD parameters and catalyst deposition and selecting optimal substrate materials. Also, the role of catalyst particles in nanotube growth on silicon and silicon oxide substrates will be discussed.

* To whom correspondence should be addressed. E-mail: jungy@rpi.edu (Y.J.J.; homma@will.brl.ntt.co.jp (Y.H.).

† NTT Basic Research Laboratories, Atsugi, Kanagawa 243-0198, Japan.

‡ Department of Physics, Meiji University, Higasimita, Tama-ku, Kawasaki 214-8571, Japan.

2. Experimental Details

In our experiments SWNTs are grown on patterned silicon and silicon oxide structures by the thermal CVD method using methane (CH_4) as a carbon source.[18] Figure 1 shows the schematics for designing and building SWNT networks in our experiment. For the substrate preparation Si(100) and SiO_2(300 nm)/Si(100) were patterned using synchrotron-radiation lithography as shown in Figure 1a. Patterned substrates have various shapes in submicrometer size, such as pillars (200 nm diameter and 300 nm height with a 250 nm distance between pillars) and lines (500 nm wide and a 500 nm distance between line structures). The prepared substrates were chemically cleaned in H_2O_2/H_2SO_4 (1:4) solution and subsequently rinsed with deionized water. Then Fe or Co thin films (5−10 Å thickness) were deposited as catalysts for nanotube growth using a conventional vacuum evaporator. During the catalyst film deposition, substrates were tilted twice about +45° and −45° to paste catalysts and grow carbon nanotubes on the side wall of patterned structures as well as on the top of the substrate (Figure 1b,c). For the SWNT growth, prepared substrates were placed on the carbon plate inside a quartz tube above the heater in the CVD furnace. Argon gas was supplied to prevent the substrate surface and carbon nanotubes from oxidation, and pressure was maintained around 500 Torr. After the furnace was heated to the deposition temperature of 800−950 °C, methane (CH_4) was introduced into the quartz tube as a carbon source for the carbon nanotube growth with a 300 sccm flow rate for 1−2 min. After nanotube growth, scanning electron microscopy (SEM; Hitachi S-5000; high-resolution SEM, HRSEM) was employed to observe the growth behaviors of carbon nanotubes on the designed substrates. Raman spectroscopy using a 785 nm wavelength and transmission electron microscopy (TEM; Hitachi H-9000 operated at 300 keV) were employed to characterize the structures of carbon nanotubes and catalyst particles on the patterned silicon oxide and silicon substrates. For TEM observation of carbon nanotubes, patterned substrates after CVD were scratched using a diamond scriber, and the flakes were placed on the transmission electron microscope grid. For the TEM sample preparation for cross

10.1021/jp0346514 CCC: $25.00 © 2003 American Chemical Society
Published on Web 06/21/2003

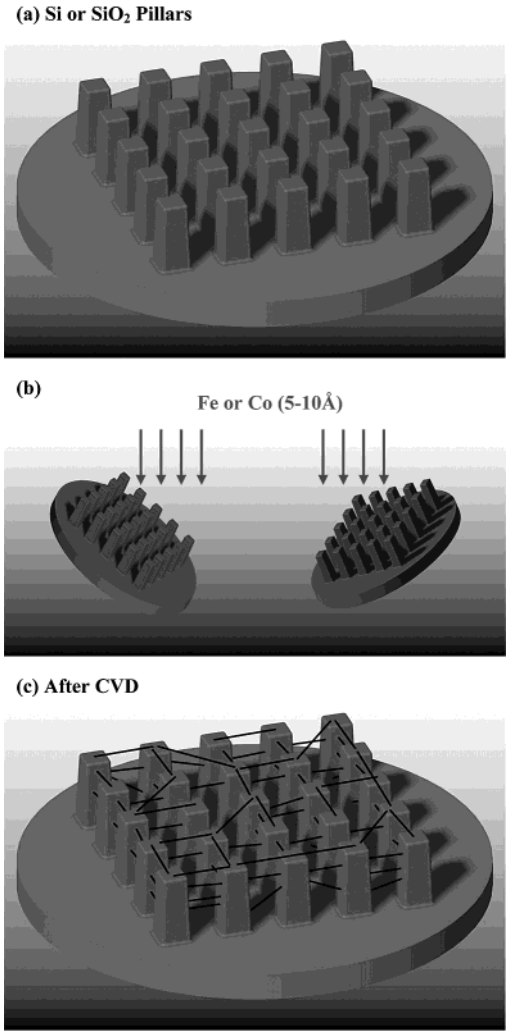

Figure 1. Schematic for designing high-density single-walled nanotube networks on patterned substrates using the CVD method: (a) preparation of submicrometer-scale patterned substrates (Si or SiO_2) by X-ray lithography; (b) thin catalyst (Fe or Co) film deposition on the 45°-tilted patterned substrate using a two-step process to cover the sides of the pillars; (c) schematic of nanotube networks bridging the pillars after CVD.

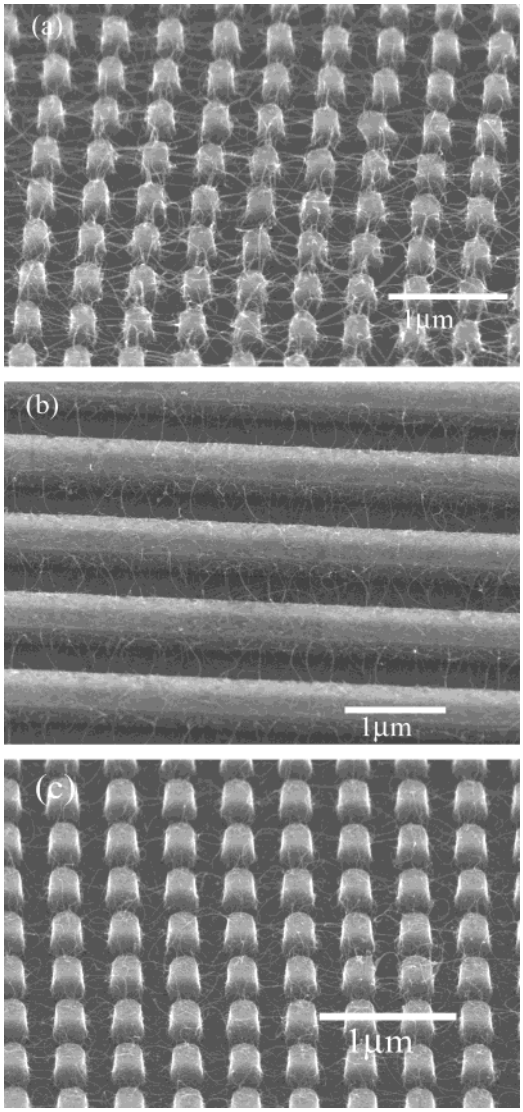

Figure 2. SEM images of single-walled carbon nanotube networks formed on variously shaped submicrometer-scale patterned silicon oxide substrates using a Fe thin-film catalyst at 900 °C: (a) high-density single-walled carbon nanotubes grown on silicon oxide pillars having a 200 nm diameter, 400 nm height, and 250 nm distance between pillars; (b) high-density single-walled nanotube networks formed on 500 nm wide silicon oxide line patterns; (c) SWNTs produced by methane CVD on patterned pillar structures.

sectional observation of catalyst particles on silicon and silicon oxide surfaces, an amorphous carbon film and subsequently a tungsten film were deposited on the surface of the interested areas to protect the surface from ion irradiation. Then, extra materials were removed from both sides of the region of interest using a focused Ga ion beam (FIB; Hitachi FB-2000A), until a very thin (electron microcopy transparent) specimen (200 nm) was obtained. Then, the thinning part was removed from the substrate and mounted on a copper grid using the "microsampling technique".[19]

3. Results

3.1. High-Density SWNT Networks on Nanoscale Patterned Structures. Figure 2 shows representative SEM images of high-density SWNT networks formed on variously shaped nanoscale silicon oxide patterns using Fe or Co catalyst. First we clearly observe that the yield of the suspended SWNT is significantly higher than that obtained by any previous method.[18,20] Figure 2a is the SEM image of SWNT networks grown on silicon oxide pillars having a 200 nm diameter, 300 nm height, and 250 nm distance between neighboring pillars using Fe catalyst at 900 °C. As shown in our schematic illustration (Figure 1b,c), since catalyst films were deposited on the side wall of pillars as well as on the top and bottom of patterned structures by tilting the substrates, most of the nanotubes not only started to grow and connect from the top of the silicon oxide pillars but also make bridges between the side walls of the pillars, therefore forming highly dense nanotube networks. Closer observation of the nanotube network structures indicates that many nanotubes are on the bottom of the substrate and they often grow along the side walls of the patterned structures. Similar suspended highly dense SWNT growth behaviors and network formations are observed using the same method on different patterns and line shapes (500 nm width and distance between lines) as shown in Figure 2b. These nanotubes in Figure 2a,b are well directed during growth and form highly organized SWNT architectures following a predesigned geometry of the patterned structures. As previously reported on suspended nanotube growth behavior on silicon pillar structures,[18] most of the carbon nanotubes make nearest-neighbor connection with

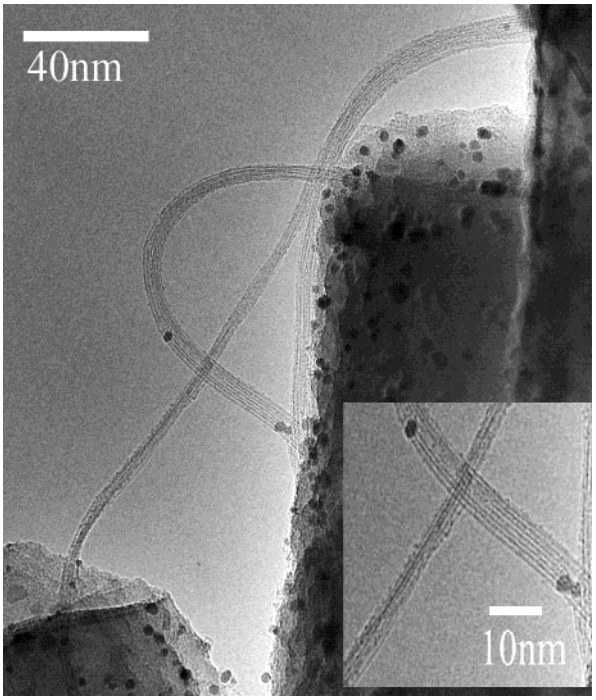

Figure 3. TEM image of single-walled nanotube networks grown on SiO_2 pillars using a Co thin-film catalyst at 800 °C.

the pillars (Figure 2a). In the case of line patterns, carbon nanotubes preferentially grow perpendicular to the direction of the line shapes (Figure 2b) regardless of the methane flow direction.

We are also able to create high-density SWNT networks using a Co catalyst film instead of Fe. Figure 2c shows the SEM image of SWNT networks formed on the same SiO_2 pillar structures using the Co thin film as a catalyst for nanotube growth. Compared to that using Fe catalyst, CVD for nanotube growth using Co catalyst could be operated at a lower deposition temperature, 800 °C, and the morphology of SWNT is similar to that of the nanotube networks fabricated by Fe catalyst at 900 °C. However, the probability to build nanotube bridges between patterns spaced at larger distances was observed to be much lower; this might be due to the lower growth temperature, compared to that of the SWNT grown by Fe catalyst.

A TEM observation of carbon nanotubes on pillar structures (Figure 3) showed that bundles of SWNTs with 1−1.3 nm diameters were produced by our method. We could observe that catalyst particles (Fe; 3−7 nm size) are formed all over the patterned structures. Also the TEM image in Figure 3 clearly reveals that SWNT bundles grown from catalyst particles on the patterned pillar structures are connecting neighboring pillars, forming nanotube bridges.

3.2. Roles of CVD Parameters and Catalyst Particle Sizes for High-Density SWNT Growth. Our approach for building high-density SWNT networks involved selecting optimal substrates and controlling CVD parameters such as the growth temperature, the flow rate of methane (CH_4), and the size of the catalyst particles. In our experiment, we found that growing SWNTs is strongly dependent on the temperature and the size of the catalyst particles during CVD. Temperatures in the range of 800−900 °C and catalyst (Fe, Co) particle sizes in the range 3−7 nm are necessary to obtain high-density SWNT growth. Figure 4 shows the strong temperature effect seen for SWNT growth on bare silicon(100) substrate using the thin-film Fe catalyst. As shown in Figure 4a, when the growth temperature is lower than 800 °C, the probability of SWNT growth becomes

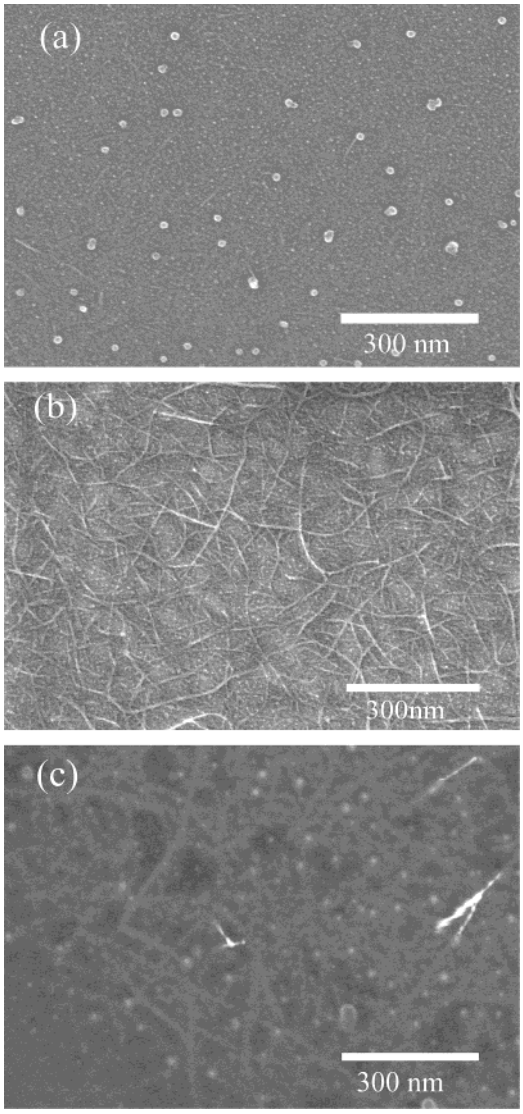

Figure 4. SEM images after methane CVD on a silicon(100) surface using a thin Fe film catalyst showing temperature dependence for high-density single-walled carbon nanotube growth at (a) 800 °C, (b) 900 °C, and (c) 950 °C.

low even with very small catalyst particles; multiwalled carbon nanotubes (MWNTs) are easily produced from large Fe catalyst particles (50−100 nm) at this temperature.[20] At around 900 °C we could observe highly dense SWNT growth on the silicon surface (Figure 4b). However, as shown in Figure 4c, above 950 °C SWNTs were rarely formed.

The size of the catalyst particles is also very crucial to produce high-density SWNTs. When a thick catalyst film (>10 Å) was deposited and used for nanotube growth, relatively large catalyst particles were formed during CVD and the yield of SWNTs was low compared to that for a thin catalyst film (<10 Å) forming small catalyst particles during CVD. Therefore, by simply depositing a thin catalyst film with an around 5−10 Å thickness, we could obtain very small catalyst particles with 3−7 nm sizes after CVD for high-density SWNT growth.

The yield of SWNT was not affected by methane flow rates between 100 and 700 sccm. However, in a methane flow rate less than 100 sccm at 500 Torr, the yield of SWNT was low.

3.3. Effect of Substrate on SWNT Growth. Figure 5 shows SEM results of highly directional growth of SWNT networks on different substrate materials such as Si and SiO_2. Top views of the SWNT network grown with the same CVD parameters

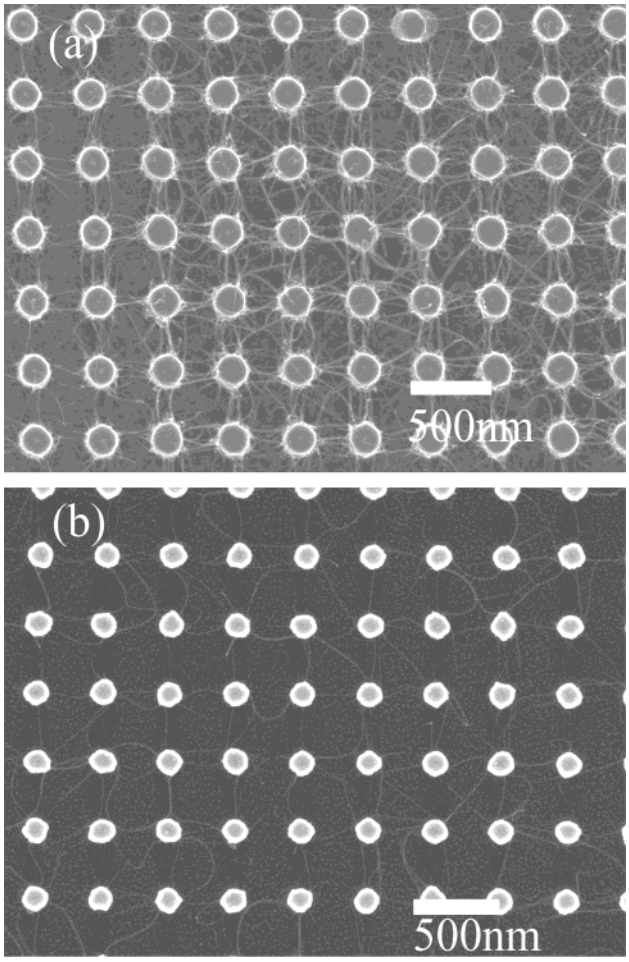

Figure 5. Top views of single-walled nanotube networks formed on different substrate materials, with the same CVD parameters, showing strong substrate dependence for high-density single-walled carbon nanotube growth: (a) silicon oxide pillar substrate; (b) silicon pillar substrate.

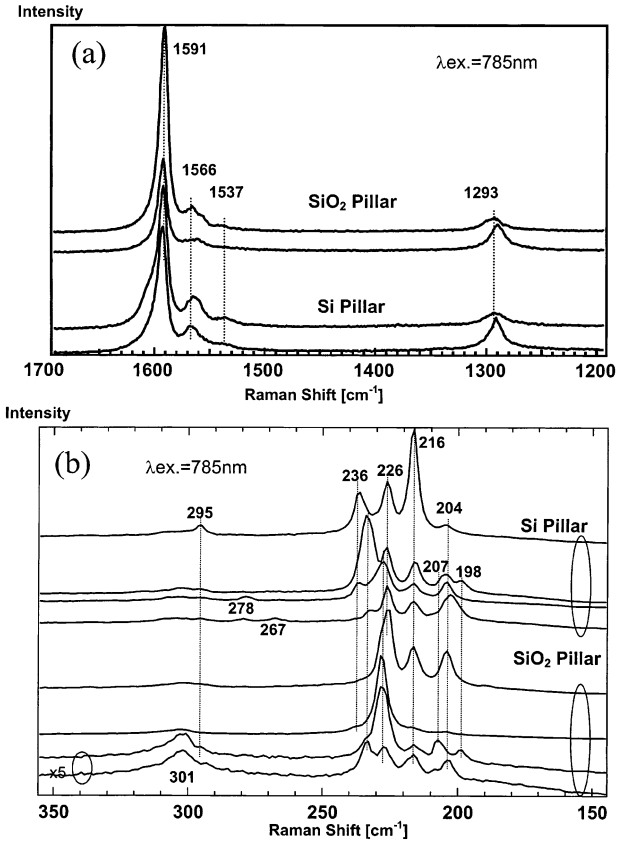

Figure 6. Micro-Raman spectra (using a 785 nm wavelength laser probe) from SWNT networks on nanoscale patterned silicon and silicon oxide pillars: (a) spectral range between 1200 and 1700 cm^{-1} where G- and D-bands are observed; (b) low-frequency range of Raman spectra at the RBM region. Each spectrum was taken from different positions on the SiO_2 or Si pillar samples by scanning the laser probe beam at an interval of several micrometers.

on SiO_2 nanopillars (Figure 5a) and Si nanopillars (Figure 5b) clearly show that there is a very strong substrate dependence of the SWNT yield. When comparing silicon and silicon oxide pillar substrates for nanotube growth, we find that the density of SWNTs on silicon oxide pillar structures shown in Figure 5a is much higher than that on silicon pillar structures in Figure 5b. The observations show the formation of larger sized SWNT bundles on the patterned SiO_2 pillar substrate compared to the smaller sized SWNT bundles on the patterned Si substrate. The same difference is also observed on differently shaped patterns by SEM observation.

We have used Raman spectroscopy for obtaining structural information on the SWNTs bridging between the nanopillars on differently patterned substrate materials. Raman signals from the suspended SWNTs can be measured selectively since the signal intensities from nanotubes grown on the flat region of the substrates are much weaker than these from the suspended SWNTs.[21] Figure 6 compares typical Raman spectra obtained from SWNTs grown on SiO_2 and Si pillar structures. A series of spectra were taken from different positions on the SiO_2 or Si pillar samples by scanning the laser probe beam using the mapping equipment at an interval of several micrometers. The probe beam was about 1 μm in diameter with a wavelength of 785 nm (1.58 eV). A spectral range of 1200−1700 cm^{-1}, assigned to the G-bands and the D-bands, was observed.[22] The G-band around 1590 cm^{-1} is ascribed to the tangential modes of the graphite structure, and the D-band is a disorder-induced band at around 1290 cm^{-1} and is activated by the presence of defects or by the finite size of the nanotube. It can be seen from Figure 6a that the frequencies of these G- and D-bands are practically the same, not depending on the materials constituting the pillars. This result means that there are very few differences between nanotube structures (including the cluster size of the graphene sheets and tube diameter) grown on Si and SiO_2 pillars.[23,24] Typical low-frequency Raman spectra at the radial breathing mode (RBM) region obtained under conditions similar to those of Figure 6a are presented in Figure 6b. The RBM signals from the suspended SWNTs grown between the pillars of Si and SiO_2 are observed in the frequency range of 198−236 cm^{-1}. The diameter of an isolated SWNT is calculated from d (nm) $= A/[\omega_R$ (cm^{-1}) $- 14]$,[25] where d is the isolated SWNT diameter, A is a proportionality constant, and ω is the RBM frequency. Several values have been reported for A, and among them, widely used values in recent literature are 224[26] or 248.[27] Therefore, the observed frequency range of the RBM signals corresponds to an SWNT diameter of 1.05−1.25 nm (for $A =$ 248) for individual nanotubes or 1.01−1.27 nm (for $A = 224$) for bundled nanotubes. In Figure 6b, Raman bands from at least eight different types of semiconducting SWNTs are observed, and signals due to metallic ones are hardly observed. These RBM bands are nearly identical on both Si and SiO_2 pillars.

4. Discussion

The SWNT growth process we used to construct nanotube networks described above is based on thermal CVD. This

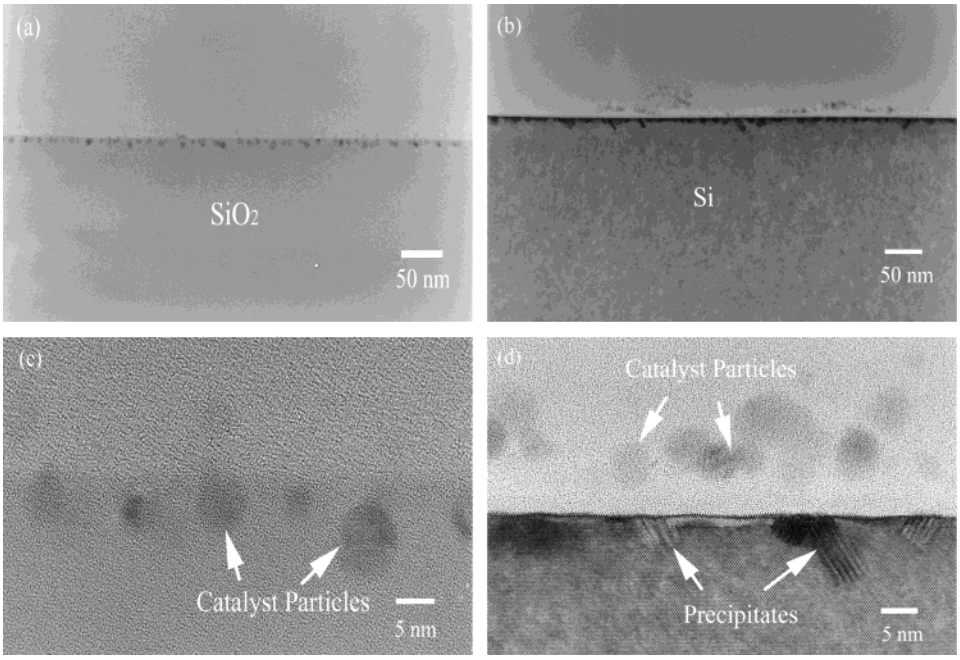

Figure 7. TEM images of the cross section of the substrates: (a) SiO_2 substrate after CVD; (b) Si substrate after CVD showing precipitation of submicrometer-sized particles near the Si surface; (c) enlarged picture from (a) showing partially embedded active catalyst particles as indicated with arrows; (d) enlarged area from (b) showing both catalyst particles and the formation of compound crystals (arrows) near the Si surface during CVD processing.

method uses methane as a carbon source and a predeposited Fe or Co thin film as a catalyst on patterned silicon or silicon oxide substrates. The technique mainly involves deposition of a very thin metal catalyst film (Fe or Co) on nanoscale designed patterns without any presurface treatments and/or without any chemical pretreatments of catalysts, which have been used to confine the size of catalyst particles for SWNT growth.[17,28,29] At high growth temperatures (800−900 °C) during CVD, these thin catalyst films (5−10 Å) are thermally destroyed and directly form small catalyst particles (3−7 nm) that can effectively prompt the growth of SWNTs on the substrate.

Another important result in our experiment is the strong dependence of SWNT growth on substrate materials. Some researchers have already reported the importance of catalyst support materials for nanotube growth.[30,31] In our experiment we note that there is a significant difference in the density of SWNTs between silicon and silicon oxide patterned substrates. To understand the growth mechanism of SWNTs on different substrate materials (Si and SiO_2), we have performed TEM observations of catalyst particles on silicon and silicon oxide substrates. Information on these Fe catalyst particles after nanotube growth can be obtained from cross sectional TEM observation of bare silicon and silicon oxide substrates shown in Figure 7. On the SiO_2 area, we can easily observe that the catalyst particles are partially embedded into the SiO_2 matrix (Figure 7a). An enlarged TEM image of the SiO_2 area (Figure 7c) shows irregularly shaped particles 3−7 nm in diameter. While focused on the Si area, we find crystallized precipitates formed with well-defined shapes inside the silicon matrix (Figure 7b,d) as well as irregularly shaped catalyst particles above the silicon surface similar to those in Figure 7c. We do not yet have a clear understanding of the discriminating factors that form small catalyst particles and precipitates. However, these observations seem similar to our recent results showing the mechanism of the site selectivity of MWNT growth on SiO_2/Si patterned substrate using the vapor-phase catalyst delivery method (ferrocene/xylene).[32] In our previous experiment we found active γ iron (γ-Fe) catalyst particles effectively promoting MWNT growth on the SiO_2 surface. We also found iron silicide ($FeSi_2$)/iron silicate (Fe_2SiO_4) particles beneath the silicon surface during the high-temperature deposition process, creating catalytically inactive Fe compounds, resulting in no nanotube growth.[33] In our SWNT synthesis process, it is assumed that on the SiO_2 region most of the particles from the thin Co or Fe film exist as a stable catalyst effectively decomposing methane and supplying carbon species for SWNT formation. However, on the Si area there might be a chemical reaction (thereby creating catalytically ineffective compounds) between silicon and the catalyst by diffusion of Fe or Co through the native SiO_2 at high temperature.[34]

5. Conclusion

SWNTs were grown on nanoscale patterned Si and SiO_2 structures using the thermal CVD method. The method provides a very simple and effective way to build highly dense self-assembled SWNT networks on nanostructured substrates. The high-yield growth of nanotube networks is obtained by controlling the deposition of a thin-film catalyst, optimizing the CVD parameters (particularly the growth temperature), and selecting optimal substrates for which Fe or Co particles remain as active catalysts for SWNT growth.

Acknowledgment. We acknowledge funding from the NEDO International Joint Research Grant Program, the Focus Center New York for Electronic Interconnects at Rensselaer Polytechnic Institute (RPI), the RPI NSF NSEC on directed assembly of nanostructures, and Philip Morris. We thank Jeremy Vosburgh at RPI for discussion.

References and Notes

(1) Dresselhaus, M. S.; Dresselhaus, G.; Avouris, P. *Carbon nanotubes: synthesis, structure, properties, and applications*; Springer: Berlin, New York, 2001.

(2) Yakobson, B. I.; Brabec, C. J.; Bernholc, J. *Phys. Rev. Lett.* **1996**, *76*, 2511.

(3) Wong, E. W.; Sheehan, P. E.; Lieber, C. M. *Science* **1997**, *277*, 1971.
(4) Falvo, M. R.; Clary, C. J.; Taylor, R. M.; Chi, V.; Brooks, F. P.; Washburn, S.; Superfine, R. *Nature* **1999**, *397*, 236.
(5) Ajayan, P. M. *Chem. Rev.* **1999**, *99*, 1787.
(6) Avouris, P. *Chem. Phys.* **2002**, *281*, 429.
(7) Appenzeller, J.; Knoch, J.; Derycke, V.; Martel, R.; Wind, S.; Avouris, P. *Phys. Rev. Lett.* **2002**, *89*, art. no. 126801.
(8) Javey, A.; Wang, Q.; Ural, A.; Li, Y.; Dai, H. *Nano Lett.* **2002**, *2*, 929.
(9) Choi, W. B.; Chae, S.; Bae, E.; Lee, J.; Cheong, B.; Kim, J.; Kim, J. J. *Appl. Phys. Lett.* **2003**, *82*, 275.
(10) Kreupl, F.; Graham, A. P.; Duesberg, G. S. Steinhogl, W.; Liebau, M.; Unger, E.; Honlein, W. *Microelectron. Eng.* **2002**, *64*, 399.
(11) Lee, Y.; Jang, Y.; Choi, C.; Kim, E.; Ju, B.; Kim, D.; Lee, C.; Yoon, S. *J. Appl. Phys*. **2002**, *91*, 6044.
(12) Wei, B. Q.; Zhang, Z. J.; Ramanath, G.; Ajayan, P. M. *Appl. Phys. Lett.* **2000**, *77*, 2985.
(13) Kong, J.; Franklin, N. R.; Zhou, C.; Chapline, M. C.; Peng, S.; Cho, K.; Dai, H. *Science* **2000**, *287*, 622.
(14) Wei, B. Q.; Vajtai, R.; Ajayan, P. M. *Appl. Phys. Lett.* **2001**, *79*, 1172.
(15) Frank, S.; Poncharal, P.; Wang, Z. L.; De Heer, W. A. *Science* **1998**, *280*, 1744.
(16) Cassell, A. M.; Franklin, N. R.; Tombler, T. W.; Chan, E. M.; Han, J.; Dai, H. *J. Am. Chem. Soc*. **1999**, *121*, 7975.
(17) Franklin, N. R.; Dai, H. *Adv. Mater*. **2002**, *12*, 890.
(18) Homma, Y.; Kobayashi, Y.; Ogino, T.; Yamashita, T. *Appl. Phys. Lett*. **2002**, *81*, 2261.
(19) Ohnishi, T.; Koike, H.; Ishitani, T.; Tomimastsu, S.; Umemura, K.; Kamino, T. *Proceeding of the 25th International Symposium for Testing and Failure Analysis*, Santa Clara, 1999; p 449.
(20) Homma, Y.; Yamashita, T.; Finnie, P.; Tomita, M.; Ogino, T. *Jpn. J. Appl. Phys*. **2002**, *41*, 89.
(21) Kobayashi, Y.; Homma, Y.; Ogino, T. To be submitted for publication.
(22) Dresselhaus, M. S.; Eklund, P. C. *Adv. Phys.* **2000**, *49*, 705.
(23) Pimenta, M. A.; Jorio, A.; Brown, S. D. M.; Souza, A. G.; Dresselhaus, G.; Hafner, J. H.; Lieber, C. M.; Saito, R.; Dresselhaus, M. S. *Phys. Rev. B* **2001**, *64*, art. no. 041401.
(24) Ferrari, A. C.; Robertson, J. *Phys. Rev. B* **2000**, *61*, art. no. 14095.
(25) Rao, A. M.; Chen, J.; Richter, E.; Schlecht, U.; Eklund, P. C.; Haddon, R. C.; Venkateswaran, U. D.; Kwon, Y. K.; Tomanek, D. *Phys. Rev. Lett.* **2001**, *86*, 3895.
(26) Bandow, S.; Asaka, S.; Saito, Y.; Rao, A. M.; Grigorian, L.; Richter, E.; Eklund, P. C. *Phys. Rev. Lett.* **1998**, *80*, 3779.
(27) Jorio, A.; Saito, R.; Hafner, J. H.; Lieber, C. M.; Hunter, M.; McClure, T.; Dresselhaus, G.; Dresselhaus, M. S. *Phys. Rev. Lett*. **2001**, *86*, 1118.
(28) Colomer, J. F.; Stephan, C.; Lefrant, S.; Van Tendeloo, G.; Willems, I.; Konya, Z.; Fonseca, A.; Laurent, Ch.; Nagy, J. B. *Chem. Phys. Lett.* **2000**, *317*, 83.
(29) Delzeit, L.; Chen, B.; Cassell, A.; Stevens, R.; Nguyen, C.; Meyyappan, M. *Chem. Phys. Lett.* **2001**, *348*, 368.
(30) Kong, J.; Cassell, A.; Dai, H. *Chem. Phys. Lett.* **1998**, *292*, 567.
(31) Cassell, A.; Raymakers, J.; Kong, J.; Dai, H. *J. Phys. Chem*. **1999**, *103*, 6484.
(32) Wei, B. Q.; Vajtai, R.; Jung, Y.; Ward, J.; Zhang, R.; Ramanath G.; Ajayan, P. M. *Nature* **2002**, *416*, 495.
(33) Jung, Y. J.; Wei, B. Q.; Vajtai, R.; Ajayan, P. M.; Homma, Y.; Prabhakaran, K.; Ogino, T. *Nano Lett.* **2003**, *3*, 561.
(34) Chemelli, C.; D'Angelo, D.; Girardi, G.; Pizzini, S. *Appl. Surf. Sci.* **1993**, *68*, 173.